# Two-Component System Cycloheptanol (C7) + Cyclooctanol (C8): An Extraordinary System

**M. A. Rute,[†] J. Salud,[†] P. Negrier,[‡] D. O. López,*[,†] J. Ll. Tamarit,[†] R. Puertas,[†] M. Barrio,[†] and D. Mondieig[‡]**

*Laboratori de Caracterització de Materials (LCM), Departament de Física i Enginyeria Nuclear, E.T.S.E.I.B., Universitat Politècnica de Catalunya. Diagonal, 647 08028 Barcelona, Spain, and Centre de Physique Moléculaire, Optique et Hertzienne UMR 5798 au CNRS-Université Bordeaux I351, cours de la Libération, 33405 Talence Cedex, France*

*Received: October 7, 2002*

The two-component system cycloheptanol (C7) + cyclooctanol (C8) has been studied by means of thermal analysis, X-ray powder diffraction, and dielectric spectroscopy. In a first step, the polymorphism of pure C7 and C8 has been revised, and new unpublished crystallographic data of the stable phases have been reported. Evidence for the isomorphism relationship between the simple cubic (SC) phases of both of the pure components has been seen through the continuous evolution of the lattice parameters, the continuous evolution of the dielectric strength, and the existence of a two-phase equilibrium [SC + L]. Despite the solid polymorphism of the pure components, the SC state has been observed to be the sole mixed solid state between 170 K and [SC + L] equilibrium. To perform a complete thermodynamic analysis, measurements of the excess enthalpy in the liquid state were undertaken. These measurements together with the experimental melting-phase diagram allow us to determine the excess thermodynamic properties of the mixed SC state via a compensation law. Dielectric data have been used to interpret the excess properties, and the existence of short-range orientatonal order for the mixed SC state has been inferred. In addition, this OD mixed state has been classified as extraordinary in light of the log $T_C$−log $T_m$ plot.

## 1. Introduction

Cyclic alcohols are of interest because their different molecular conformations might lead not only to a complex polymorphism but also to glass transitions. Cyclooctanol (C8) and cycloheptanol (C7) are two representative examples that exhibit a rich polymorphism in the solid state, but the number of stable solid phases and their lattice symmetries seem not to be fully clarified.

As far as C8 is concerned, some work was carried out to study its stable polymorphism and also its glass/glassy behavior. Actually, this work is relative to differential thermal analysis (DTA) at normal or high pressure,[1,2] dielectric measurements also at normal or high pressure,[3−9] adiabatic calorimetry,[10] thermal conductivity,[11] and NMR spectroscopy[1]. Surprisingly, no studies relating X-ray diffraction, as far as we know, are reported—only the symmetry of the phase for the melts was reported to be face-centered cubic, the lattice parameter being 9.56 Å.[12] Edelmann and Würflinger[2] reported two stable solid phases at normal pressure, denoted on cooling from the liquid state as phase I and phase II. Afterward, other authors[6,11] confirmed these two solid phases, and in addition, they inferred the existence, by thermal conductivity experiments, of a new stable phase at normal pressure below 220 K, denoted as phase III. Nevertheless, more recently, Sciesinski et al.[10] were unable to obtain phase III by adiabatic calorimetry. The possibility that phase III is a consequence of the impurity of the compound was considered by some of the authors that inferred it.[11] It seems to be doubtless that phase I is orientationally disordered (OD) from dielectric[6−9] and NMR[13] measurements. The disorder in this OD state must be described as being due to quasi-isotropic or endospherical reorientations, which means that the molecules reorient around three different axes. As far as phase II is concerned, Dworkin et al.[1] argued that there exists some kind of disorder that can become frozen in to yield a glassy state. This was newly stated 13 years later by Sciesinsky et al.[10] As for phase III, if it exists as a stable phase, it was considered to be an ordered crystalline phase. The possible existence of phase III was earlier inferred by Dworkin et al.[1] from the existence of a glass transition in phase II.

As for C7, its solid polymorphism has been studied by means of several techniques: thermal analysis,[9,15,16] dielectric spectroscopy,[9,16,17] IR absorption,[14,15] and Raman spectroscopy.[15] As far as we know, no X-ray diffraction studies are reported. From the work of Adachi et al. in 1972,[15] eight different solid phases were stated, the stable phases being only four. They were denoted on cooling from the liquid state as phase I, phase II, phase III, and, strangely, phase II′. In fact, phase II′ should be called phase IV. The stability of all of these phases was stated by means of Gibbs energy calculations from specific heat experimental values. Nevertheless, Poser et al. in 1985[16] studied C7 by means of DTA, and only three stable phases on decreasing temperature from the liquid state, denoted as I, II, and III (in the same way as Adachi et al.[15]), were observed. In addition, several metastable phases depending on the annealing conditions were reported. Moreover, very recently, Tyagi and Murthy[9] in the same way as Adachi et al.[15] not only speak on four stable phases but also report that each phase seems to have an

* To whom correspondence should be addressed. E-mail: david.orencio.lopez@upc.es.
[†] Universitat Politècnica de Catalunya.
[‡] Université Bordeaux I351.

10.1021/jp022193d CCC: $25.00 
Published on Web 05/24/2003

associated glassy state. From this work, all four phases are reported to be OD. Sciesinska et al.[14] considered that only phases I, II, and III are OD, whereas phase IV has an orientational disorder of the static type. Poser et al.[16] by dielectric spectroscopy considered that only phases I and II are expected to be OD because of high values of the static permittivity.

The OD phases in pure components and in binary mixed crystals were the subject matter of the authors in the last 15 years. The work was and is presently addressed to both structural and thermodynamic properties.

In this paper, we present the results of thermodynamic, dielectric spectroscopy, and structural investigations on the binary system C7 + C8. The thermodynamic data pertain to the liquid state and to the melting of the mixed OD state and allow us to calculate the excess enthalpy and excess entropy of the mixed crystals' OD. Both the structural and dielectric spectroscopic data are obtained for the mixed OD state and for phase I of the pure components. The principal aim of the paper is to examine to what extent the available data will allow a description of the molecular mixed state (intermolecular interaction network and the order/disorder phenomena).

In more detail, the actions to be taken are the following. First, a preliminary study of the polymorphism of pure C7 and C8 was made to determine the melting phase diagram of the two-component system C7 + C8. Evidence for the existence of an isomorphism relationship in the OD state (a continuous series of OD mixed crystals) has been seen from X-ray powder diffraction, thermal analysis, and dielectric spectroscopy. Afterward, the measured excess enthalpy of the liquid state was used to determine the excess properties of the OD mixed crystals through a complete thermodynamic analysis in which a compensation law was considered. Spectroscopic data of the dielectric strength in the mixed OD state were used to interpret the hidden information held in the thermodynamic excess properties.

The paper is organized as follows. In section 2, we describe the experimental details. In section 3, the observed stable polymorphism of C7 and C8 is presented. In section 4, the experimental melting phase diagram along with the dielectric data is depicted. In section 5, a complete thermodynamic analysis for which experimental mixing enthalpies of the liquid state are measured is carried out. In section 6, a discussion is performed, and finally, in section 7, we summarize the main conclusions.

## 2. Experimental Section

**2.1. Materials.** Cyclooctanol and cycloheptanol were obtained from Across Organics with purities higher than 99% and were purified by means of several sublimation and crystallization processes. Both compounds were always handled with extreme caution in an Ar-controlled atmosphere. The binary mixtures were prepared in the liquid state by mixing both pure components in the selected proportions.

**2.2. Thermal Analysis.** Thermal properties of the phase transitions (temperatures and enthalpy changes) in the pure components and the binary mixtures were determined by means of a Modulated DSC TA2920 system from TA Instruments Inc. equipped with a cooling accessory. Heating and cooling rates of 2 $K \cdot min^{-1}$ and sample masses of about 10 mg were used. The DSC signals were interpreted according to the shape factor method, the details of which can be found elsewhere.[18,19]

**2.3. Mixing Calorimetry.** The excess enthalpy in the liquid state was obtained by means of a commercial Biocalorimètre B. C. P. from electronique Arion for which a homemade mixing-cells device was manufactured. The calorimeter (Figure 1) is designed as a high-sensitivity DTA, with two cell volumes of about 10 $cm^3$ that can work in an isothermal mode. The cell device design was made to avoid vaporization of the liquids. The liquids to be mixed are separately introduced into the sample cell (a and b in Figure 1) and isolated from one another by means of a separation membrane (c). In both cells, sample and reference, there exists an axis-centered Teflon−metal rod (d), which is moved and controlled from outside by means of a rotatory magnetic transmission device (e). Initially, the rod (d) in both cells translates along its vertical axis slowly enough to avoid turbulence until the membrane is perforated. Once this takes place, the translation movement is transformed into a rotational one to facilitate the mixing process. To avoid undesirable thermal effects produced by the mechanical device, identical conditions are used in both cells, the liquid being self-mixed in the reference cell.

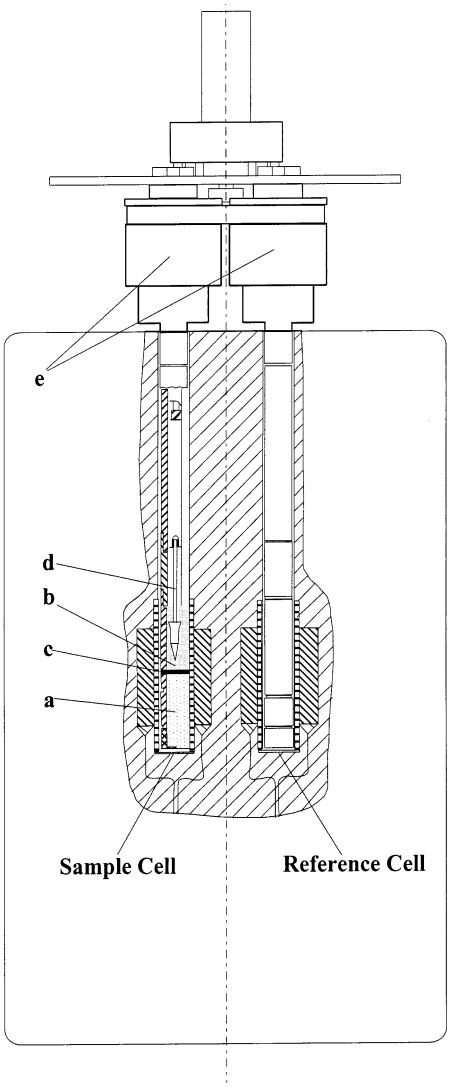


**Figure 1.** Schematic mixing-cells device for the measurement of the enthalpy of mixing of liquids. a and b are the lower and upper cavities, respectively. c is the separation membrane. d is the Teflon−metal rod. e is the magnetic-rotatory transmission device.

Before and after recording the mixing curve, a steady state corresponding roughly to the extreme of the curve was established. Electrical calibration was done by superposing a Joule effect on the sample cell in the mixing curve. The calibration constant of about 40 $mV \cdot mW^{-1}$ was proven to be temperature-independent.

**TABLE 1: Phase-Transition Temperatures and Their Enthalpy Changes for Cycloheptanol (C7) and Cyclooctanol (C8)**

| compound | $T_{III-II}$ (K) | $\Delta H_{III-II}$ (kJ·mol$^{-1}$) | $T_{II-I}$ (K) | $\Delta H_{II-I}$ (kJ·mol$^{-1}$) | $T_{I-L}$ (K) | $\Delta H_{I-L}$ (kJ·mol$^{-1}$) | reference |
|---|---|---|---|---|---|---|---|
| C7 | 227.3 | 0.55 | 258.5 | 0.88 | 280.3 | 1.60 | 15 |
| | 229 | 0.55 | 250.5 | 0.85 | 278.4 | 1.60 | 16 |
| | 225.0 | | 253.6 | | 276.6 | | 9 |
| | 227.9 | 0.45 | 250.4 | 0.78 | 278.3 | 1.51 | this work |
| C8 | | | 246.5 | 1.69 | 283.8 | 1.97 | 1 |
| | | | 264.1 | 2.67 | 297.5 | 2.04 | 2 |
| | | | 258.2 | | 291.2 | | 9 |
| | | | 264.1 | 2.05 | 297.1 | 1.97 | this work |

The performance of the experimental device was successfully tested by measuring mixtures of the system cyclohexane + benzene at 298.15 K.[20]

**2.4. X-ray Powder Diffraction.** X-ray powder diffraction data were collected using a horizontally mounted INEL cylindrical position-sensitive detector (CPS-120) equipped with a liquid nitrogen INEL CRY950 cryostat (80−500 K). The detector, used in Debye−Sherrer geometry, consisted of 4096 channels, and the angular step was 0.029° ($2\theta$). Monochromatic Cu K$\alpha_1$ radiation was selected. The samples were introduced into 0.5-mm diameter Lindemann glass capillaries and were rotated around the $\theta$ axis during the experiments. External calibration using cubic-phase $Na_2Ca_3Al_2F_4$ was performed to convert channels to ($2\theta$) degrees by means of cubic spline fittings to correct the deviation from angular linearity in PSD. DIFRACTINEL software was used for the calibration and for the peak position determinations after pseudo-Voigt fittings of the standard measurements.

**2.5. Dielectric Spectrosopy.** Measurements of the static permittivity were performed with an alpha impedance analyzer ($10^{-2}$−$10^6$ Hz) from Novocontrol. The cell consists of two gold-plated brass electrodes (diameter 10 mm) separated by two 50-$\mu$m-thick silica spacers making a plane capacitor. The cell was held in a cryostat, which screens the system, and both the temperature and the dielectric measurements were fully computer-controlled by means of WINDETA software from Novocontrol. Prior to the measurements, the experimental device was calibrated by means of an impedance measurement system based on the ALPHA Dielectric Analyzer from Novocontrol. The calibration proved to be useful for dielectric samples with high and low impedance within the frequency range of the experimental device.

To perform the dielectric measurements, the materials were introduced in the liquid state into the dielectric cell. Likewise, to prevent the possibility of hole formation in the interelectrode space, an additional mechanical device was used. The data were collected in isothermal mode with a temperature stabilization of ±0.2 K.

## 3. Pure Components

Figure 2A shows a DSC thermogram of pure C8 on cooling from room temperature to 170 K and the subsequent heating at 2 K·min$^{-1}$. It should be clearly noted that on cooling the solid phase that crystallizes, phase I in Figure 2A, remains up to 170 K. Upon further heating, an exothermic effect assumed to correspond to the transition from phase I to phase II is observed, followed by two endothermic effects. The lower-temperature endothermic peak has been assigned to the phase II-to-phase I transition because the associated temperature is similar to that reported in the literature. Likewise, the higher-temperature endothermic peak has been assigned to the melting. The temperatures and enthalpy changes of both phase transitions are reported in Table 1 along with the most representative values consigned in the literature. It should be pointed out that on cooling back after phase II has been formed no thermal event was detected, proving that if phase III exists the transition to this phase may be difficult to obtain.

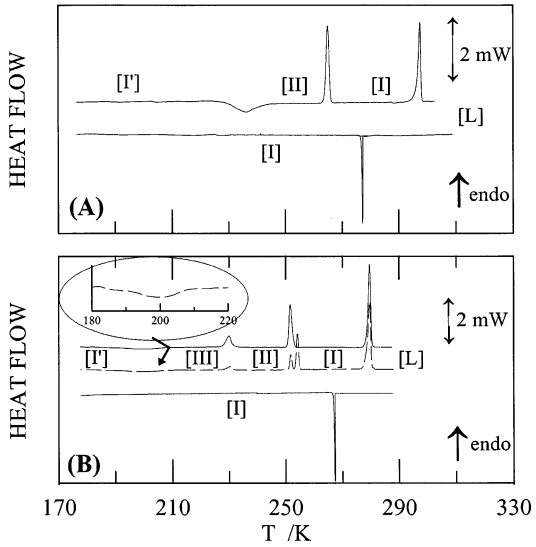


**Figure 2.** Heating and cooling DSC curves for C8 (A) and C7 (B). [I′] stands for supercooled phase I.

In summary, only two different solid phases have been found, and no indication of the existence of phase III has been obtained by means of DSC above 170 K.

Figure 2B shows a DSC thermogram of pure C7 obtained under the same conditions as that for C8. The behavior on cooling is similar to that found for pure C8 (i.e., phase I is undercooled up to 170 K). Nevertheless, the behavior on further heating (dashed line in Figure 2B) is slightly different. There are one exothermic and three endothermic effects, one of them being unfolded. Three stable solid phases seem to exist: phase III, phase II, and phase I. Following the procedure proposed by Poser et al.,[16] an annealing at 220 K for about 24 h was carried out to check the unfolded peak and the stability of these phases. The continuous line at the top of Figure 2B represents the heating after the annealing, and it provides us with a coherent picture of the stable polymorphism above 170 K. Our results together with that reported in the literature have been consigned in Table 1. As a conclusion, for pure C7, three different stable solid phases have been found above 170 K. It should be noticed, according to Adachi et al.,[15] that another stable solid phase, named phase IV, should exist below 170 K.

Figure 3 shows the X-ray powder profiles for a short $2\theta$ range of the C8 and C7 at several temperatures. They have been obtained from more than one independent experiment in which the sample was cooled and heated slowly enough to try to avoid undesirable metastabilities. As for C8, only two different phases can be inferred from Figure 3A. The upper pattern (Figure 3A) has been identified with phase I, and the lower one has been identified with phase II because the transition temperature from

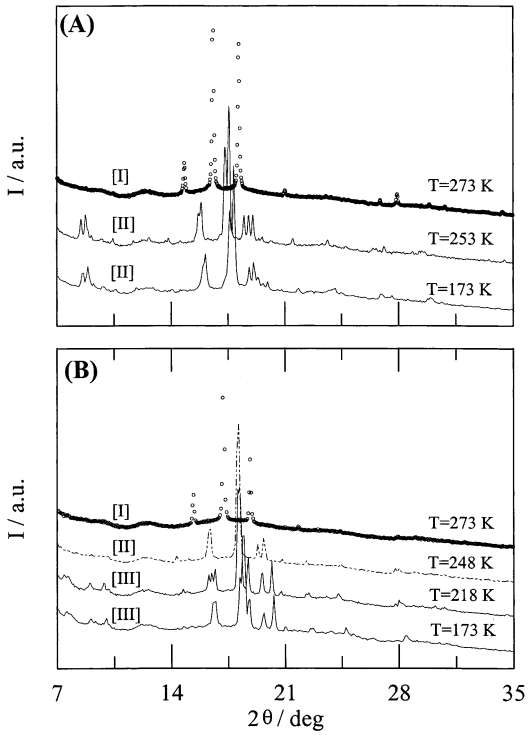


**Figure 3.** X-ray diffraction profiles for C8 (A) and C7 (B) at several temperatures.

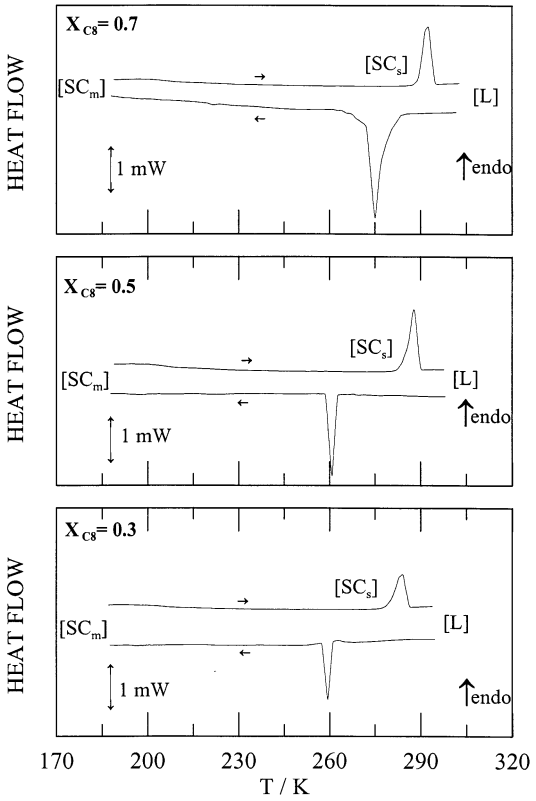


**Figure 4.** Heating and cooling DSC curves for three representative binary mixtures of the two-component system C7 + C8. [$SC_S$] stands for the stable SC state, and [$SC_m$] stands for the supercooled SC state.

phase II to phase I matches that provided by thermal analysis. The X-ray profile of phase I has been indexed by means of the DICVOL91 program[21] according to a simple cubic (SC) unit cell (M(9) = 70.5; F(9) = 58.0). Least-squares refinement (nine unambiguous reflections) of the unit-cell parameter yields 11.96(1) Å at 273 K ($Z = 8$). It is impossible to index the pattern as face-centred cubic. Likewise, the X-ray profile corresponding to phase II remains up to 170 K, and all attempts to index it have been unsuccessful, probably because of the large associated lattice. Anyway, it seems to be that the lattice symmetry of phase II should be lower than tetragonal. This would imply that in phase II the molecules undergo jumps between distinguishable orientational positions around one axis.

As for the pure C7 component, the X-ray profiles at four temperatures are shown in Figure 3B. Three different solid phases can be identified above 170 K, for which their transition temperatures are consistent with those obtained from thermal measurements. Phase I has been indexed using the DICVOL91 program as simple cubic (SC) (M(10) = 59.0; F(10) = 44.8), the parameter being 11.54(1) Å at 273 K ($Z = 8$) after least-squares refinements from 10 unambiguous reflections. It may be underlined that the SC parameter is very close to that obtained for pure C8. Phase II has been indexed according to tetragonal symmetry by means of the DICVOL91 program (M(11) = 29.1; F(11) = 34.6). The least-squares refinements of about 11 reflections lead to unit-cell parameters of $a = 19.487(2)$ Å and $c = 11.7805(2)$ Å at 248.15 K ($Z = 24$). It is important to realize that this lattice symmetry would point out that in phase II the orientational disorder of the molecules may be similar to that presented in phase II of C8. As for phase III, the X-ray pattern is not clear enough to indicate unambiguous lattice symmetry. A possible solution would be orthorhombic with similar *a* and *c* parameters as the tetragonal solution of phase II and one slightly different *b* parameter. To confirm this symmetry, additional X-ray experiments will be undertaken.

Our static permittivity measurements of both pure components will be detailed in section 4.2, but we can anticipate that they lead to comparable results with those published for several authors.

## 4. Mixed OD State

**4.1. Experimental Melting Phase Diagram.** Differential scanning calorimetry (DSC) measurements performed on C7 + C8 mixtures allowed us to determine the transition temperatures and enthalpies. Figure 4 shows the measured DSC heat flow for three different mixtures ($X_{C8} = 0.3$, $X_{C8} = 0.5$, $X_{C8} = 0.7$) on cooling from the liquid state up to 170 K and on subsequent heating. As can be observed, irrespective of the composition, the solid phase that crystallizes on cooling remains up to 170 K, and upon further heating, no thermal effects are observed up to the melting. All attempts to avoid this supercooled metastable phase have been unsuccessful.

X-ray diffraction patterns were collected at several temperatures for various C7 + C8 mixtures. The aim of this study was two-fold: (i) to verify that, in the same way as for pure components, the phase that crystallizes on cooling is simple cubic (SC) and, in addition, that the SC OD state of C7 and C8 are related by an isomorphism relationship and (ii) to prove that the SC mixed crystals are supercooled up to 170K.

Figure 5 displays the variation of the SC lattice parameter as a function of the mole fraction at two different temperatures, 273 and 173 K. Such a Figure shows the continuity in the lattice symmetry and thus the existence of the stable SC mixed crystals for the whole concentration range. In addition, the behavior of the supercooled SC mixed crystals has been proven to be similar to that of the stable ones not only in the evidence of continuity in the lattice symmetry but also in the variation of the lattice parameter with composition. Similar behavior was found some years ago in other mixed crystals between OD compounds.[22]

An outline of the experimental stable melting phase diagram of the two-component C7 + C8 system is depicted in Figure 6.

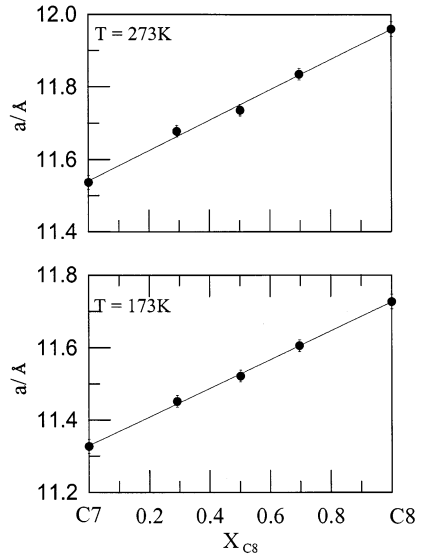


**Figure 5.** Lattice parameter *a* for SC mixed crystals of the two-component system C7 + C8 as a function of mole fraction at 273 and 173 K.

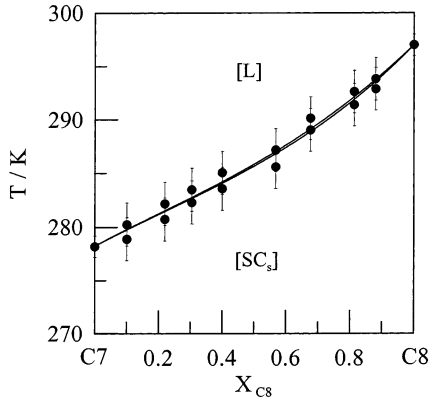


**Figure 6.** Stable melting phase diagram of the two-component system C7 + C8. The continuous line corresponds to the thermodynamically assessed phase diagram.

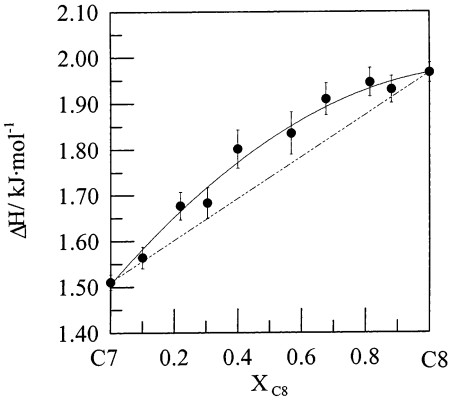


**Figure 7.** Experimental enthalpies of melting of the SC mixed crystals of the binary system C7 + C8.

As we can observe and despite the solid polymorphism of C7 and C8, the solid−solid transformations for the SC mixed crystals were not detected, and the [SC + L] equilibrium is a simple loop. The solid line in Figure 6 will be explained in section 5.3. The enthalpy change for the melting of the SC mixed crystals as a function of composition is shown in Figure 7.

**4.2. Dielectric Strength.** Figure 8 shows the dielectric strength $\Delta\epsilon$ ($= \epsilon_S - \epsilon_\infty$; $\epsilon_S$ is the static permittivity and $\epsilon_\infty$ is the permittivity at high frequency) associated with the α relaxation at 233.15 K in the OD state of pure components and four representative mixtures ($X_{C8} = 0.15$, 0.30, 0.50, and 0.70). As can be observed, the dielectric strength varies continuously between the pure components. This implies that the mixed OD state displays α-relaxation-like pure components. Likewise, the continuous variation of dielectric strength with composition is another irrefutable sign of the isomorphic character of the OD state of pure components.

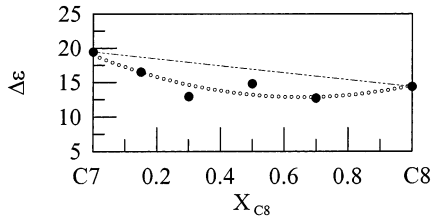


**Figure 8.** Dielectric strength $\Delta\epsilon$ for SC mixed crystals of the two-component system C7 + C8 as a function of mole fraction at 233.15 K.

## 5. Thermodynamic Analysis

**5.1. Thermodynamic Formulation and Methodology.** Under isobaric conditions, the thermodynamic properties of a binary mixture of a two-component system A + B are known if each possible phase of this mixture has an associated known molar Gibbs energy as a function of temperature and composition. The Gibbs energy function in a phase α is described by the following expression in terms of $X$ moles of B and $(1 - X)$ moles of A (i.e., the mixture $A_{1-X}B_X$):

$$G^{\alpha}(X, T) = (1 - X)\mu^{*,\alpha}_{A}(T) + X\mu^{*,\alpha}_{B}(T) + RT[(1 - X)\ln(1 - X) + X \ln X] + G^{E,\alpha}(X, T) \quad (1)$$

$\mu^{*,\alpha}_{A}$ and $\mu^{*,\alpha}_{B}$ are the molar Gibbs energies of the pure components, $R$ is the gas constant, $T$ is the thermodynamic temperature, and $G^{E,\alpha}(X, T)$ is the excess Gibbs energy that accounts for the deviation of the mixture in form α from ideal mixing behavior. Complete knowledge of expression 1 for each form is habitually unavailable, particularly because $\mu^{*,\alpha}_{A}(T)$, $\mu^{*,\alpha}_{B}(T)$, and $G^{E,\alpha}(X, T)$ are normally unknown. However, to determine and analyze a two-phase equilibrium region between two arbitrary forms α and $\beta$ in a two-component phase diagram, a simplified treatment named the equal Gibbs composition (EGC) method[23] can be used. In such a way, the difference between the Gibbs energies of the α and $\beta$ forms are zero for the EGC. This occurs for each $X$ at different temperatures, giving rise to a temperature versus composition curve, the so-called EGC curve. Setting eq 1 for the α phase equal to its parallel component for the $\beta$ phase will give the EGC curve equation

$$G^{\alpha}(X, T) - G^{\beta}(X, T) = (1 - X)\Delta\mu_{A}{}^{*}(T) + X\Delta\mu_{B}{}^{*}(T) + \Delta G^{E}(X, T) = 0 \quad (2)$$

where $\Delta\mu^{*}_{i}(T) = \mu^{*,\alpha}_{i} - \mu^{*,\beta}_{i}$ (i = A, B). To proceed further, expressions are required for $\Delta\mu^{*}_{i}(T)$ and $\Delta G^{E}(X, T)$. For $\Delta\mu^{*}_{i}(T)$, using the transition temperature as a reference point and neglecting the specific heat changes, we have

$$\Delta\mu^{*}{}_{i} \approx -\Delta S^{*}{}_{i}(T - T_i) \quad (3)$$

where $\Delta S^{*}_{i}$ is the transition molar entropy at the transition

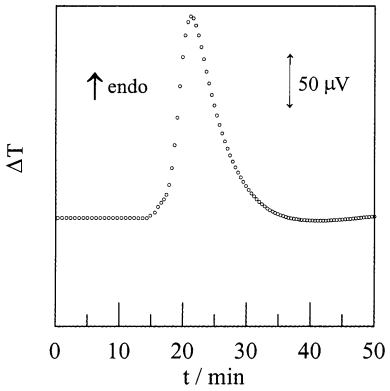


**Figure 9.** Representative mixing differential signal for mole fraction $X_{C8} = 0.6$ in the liquid state.

temperature $T_i$. Taking into account eq 3, eq 2 can be written as

$$T_{EGC}(X) = \frac{(1-X)\Delta H^*_A + X\Delta H^*_B}{(1-X)\Delta S^*_A + X\Delta S^*_B} + \frac{\Delta G^E_{EGC}(X)}{(1-X)\Delta S^*_A + X\Delta S^*_B} \quad (4)$$

The first term of the right-hand side of eq 4 is only pure component-dependent and can be obtained from pure component data. However, the second term depends on the excess Gibbs energy difference along the EGC curve. For $\Delta G^E(X, T)$, a two-parameter form of the Redlich−Kister expansion is commonly used:

$$\Delta G^E(X, T) = X(1-X)[\Delta A_1(T) + \Delta A_2(T)(1-2X)] \quad (5)$$

The $\Delta A_i(T)$ are usually taken to be constants or as a function of temperature in the form of $\Delta H_i^E - T\Delta S_i^E$.

The EGC method requires some experimental data relating to the phase transition of the mixtures in order to perform an iterative procedure in which one obtains a reasonable EGC curve and, in addition, the $\Delta G^E(X, T)$ along this curve. This procedure can be automatically carried out by means of the WINIFIT 2.0 software[24] (based upon the MS-DOS LIQFIT and PROPHASE programs[25,26]), which also allows us to calculate the different compositions at each temperature at which transitions take place, that is to say, the complete phase diagram. The program was successfully tested in other thermodynamic analyses of two-component systems.[27−29]

**5.2. Available Excess Properties of the Liquid State.** As far as we know and unfortunately, no studies of the excess properties of the liquid state of the C7 + C8 system have been reported. Thus, the excess enthalpies of six different mixtures of pure C7 and pure C8 in their liquid states have been measured by using the mixing calorimeter described above. To do so and taking into account the fact that C8 is slightly denser than C7, for each mixture, an adequate amount of C8 was put into the upper part of the sample cell, and C7 was placed into the lower part. Likewise, isothermal mixing at room temperature was observed to be difficult to produce because both compounds have high viscosities. A temperature of 323.15 K was selected to be high enough to produce good mixing. In Figure 9, one recorded isothermal trace for the mixture $X_{C8} = 0.6$ is shown as an example. As can be observed, a steady state is reached before and after the mixing of both liquids. The integrated area through the calibration constant leads to the excess enthalpy.

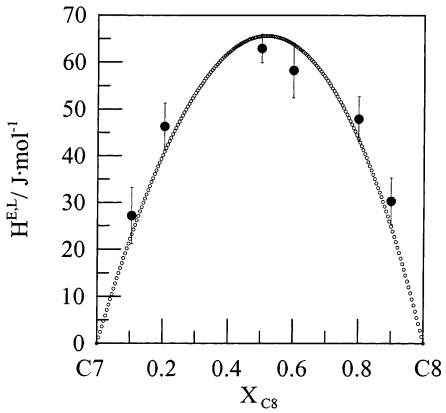


**Figure 10.** Experimental excess enthalpy in the liquid state of binary mixtures of the C7 + C8 system.

Results for excess enthalpies at various mole fractions of C8 are shown in Figure 10. At this point, we would like to draw attention to the magnitude of the measured excess enthalpy, which is about 10 times lower than that for the binary systems commonly used to calibrate such experimental systems.

The data have been fit to a two-parameter form of a Redlich−Kister polynomial:

$$H^{E,L}(X, T = 323.15\ \text{K}) = X(1-X)[262 - 19(1-2X)]\ \text{J·mol}^{-1} \quad (6)$$

These experimental mixing data, together with the melting phase diagram determined in this work (see Figure 6), enable us to obtain information about the excess properties of the SC−OD state.

**5.3. Thermodynamic Excess Properties in the OD State.** To obtain thermodynamic excess properties in the OD state, the first step is to analyze the [SC + L] two-phase equilibrium. To do so, the EGC method through eq 4, which is performed automatically by means of the WINIFIT program, needs as input (i) the data concerning the melting temperatures and entropy changes of pure components C7 and C8 and (ii) some experimental temperatures about the liquidus or the solidus of the [SC + L] loop. The output is the excess Gibbs energy change between the liquid and the SC−OD state at the mean temperature ($T_m = T_{EGC}(X = 0.5)$) of the [SC + L] loop given by a two-parameter form of a Redlich−Kister polynomial

$$\Delta G^E(X, T_m = 285.7\ \text{K}) = X(1-X)[-68.4 + 34.3(1-2X)]\ \text{J·mol}^{-1} \quad (7)$$

Equation 7 is strictly valid at $T_m$, and it seems to be temperature-independent. A simple way to take into account the temperature dependence is to adopt a quasi-subregular solution model that proved to be useful in the past for the melting of other OD mixed states.[27,30,31] In such a model, the excess Gibbs energy change can be written as

$$\Delta G^E(X, T) = X(1-X)\Delta A_1\left[1 - \frac{T}{T_C}\right][1 + \Delta A_2(1-2X)] \quad (8)$$

The constant $\Delta A_1$ expresses the change in the magnitude of the excess function. $\Delta A_2$ is a measure of its asymmetry, and $T_C$, the named compensation temperature or characteristic temperature, is defined as the ratio between the excess enthalpy change and the excess entropy change; therefore, it is the temperature at which the excess Gibbs energy change becomes zero. It is important that the followed formulation requires the assumption

that the compensation temperature must be the same for the liquid and the OD state. This assumption seems not to be an inconvenience, owing to the resemblance of both states. According to this model, the excess enthalpy change and the excess entropy change are temperature-independent and can be written as

$$\Delta H^{E}(X) = X(1 - X)\Delta A_1[1 + \Delta A_2(1 - 2X)] \quad (9a)$$

$$\Delta S^{E}(X) = X(1 - X)\frac{\Delta A_1}{T_C}[1 + \Delta A_2(1 - 2X)] \quad (9b)$$

$\Delta A_1$, $\Delta A_2$, and $T_C$ values can be derived from eq 7 in combination with data of the experimental excess enthalpy change. The latter can be calculated as an approximation, assuming that $\Delta H^{E} \approx \Delta H_m - \Delta H_{mm}$, where $\Delta H_m$ is the enthalpy of melting (see Figure 7) and $\Delta H_{mm}$ is the enthalpy change of the ideal mechanical mixture ($\Delta H_{mm} = (1 - X)\Delta H_{C7} + X\Delta H_{C8}$). The calculated $\Delta A_1$ and $\Delta A_2$ are 377 and $-18.9$ J·mol$^{-1}$ respectively.

To calculate $T_C$, the equimolar excess entropy change, considering that $\Delta G^{E}(X = 0.5, T_m) = (\Delta A_1/4) - T_m\Delta S^{E}(X = 0.5)$ is 0.390 J·mol$^{-1}$·K$^{-1}$. Thus, the ratio between the equimolar excess enthalpy change and the equimolar excess entropy change leads to a compensation temperature of 242 K, a temperature lower than $T_m$ and assumed to be the same for the liquid and SC−OD states.

The excess properties of the SC−OD state, well-represented by $A_1^{SC}$ and $A_2^{SC}$, can be read, taking into account the data of $H^{E,L}$ given by eq 6, from $A_1^{SC} = 262 - \Delta A_1$ as $-115$ J·mol$^{-1}$ and from $A_2^{SC} = -19 - \Delta A_2$ as $-0.1$ J·mol$^{-1}$. It should be noted that the asymmetry is almost negligible for the SC−OD state. The $A_1^{SC}$, $A_2^{SC}$, and $T_c$ values together with those from eq 6 have been used to calculate through the WINIFIT program the melting phase diagram of C7 + C8. The solid line in Figure 6 corresponds to the calculated melting phase diagram that fairly fits the experimental data. However, from the experimental data, a wider loop could have been expected.

## 6. Discussion

The total energy involved in the intermolecular interactions of a pure component is expressed by the lattice energy. For the studied binary system, a value of about $-50$ kJ·mol$^{-1}$ is a representative value of the lattice energy in its OD state. In a binary mixed crystal, the excess enthalpy corresponds to the difference between its lattice energy and the arithmetic mean of the lattice energies of the pure components. From the data of excess enthalpy in the OD mixed state, the effect of mixing is less than 1% of 50 kJ·mol$^{-1}$. The excess enthalpy is a fine tuning, so to speak, by the mixture of the lattice energy. In the absence of a deeper understanding of the 3D network is, it is more or less obvious that it is very difficult to propose a conclusive explanation of the signs and magnitudes of the excess properties in the OD mixed state. However, the results seem to offer some elementary expectations: (i) They do not show large excess properties, and they are rather symmetrical with regard to the equimolar composition. (ii) From the trends shown in Figures 7 and 10, the excess enthalpy of the OD mixed state is negative ($A_1^{SC} = -115$ J·mol$^{-1}$). (iii) The calculated excess entropy of the OD mixed state is also slightly negative. The assumption of the compensation between both the excess enthalpy and excess entropy leads to a virtual compensation temperature of 242 K, a value that is certainly lower than the mean temperature $T_m$ of the [OD + L] two-phase equilibrium.

Habitually, when two substances A and B form mixed crystals, positive excess enthalpy is obtained. This means that the attraction between entities A and B in a mixture is weaker than the mean of the attractions A−A and B−B in pure A and pure B, resulting in a repulsive net effect on mixing. Otherwise, the homomolecular interactions are dominant with regard to the heteromolecular ones. Nevertheless, the OD mixed state of the C7 + C8 system has a negative excess enthalpy, and thus an attraction net effect on mixing is expected as a consequence of the preponderance of the heteromolecular interactions.

Generally, the excess enthalpy has the same sign as the excess entropy, being habitually positive. Nevertheless, the excess entropy of the OD mixed state of the studied two-component system is negative. In fact, both the excess enthalpy and entropy have the same sign, thus compensating one another. In addition, the excess Gibbs energy change at $T_m$ (eq 7) leads to a negative value, giving rise to a melting two-phase equilibrium with a downward convex tendency, as can be observed in Figure 6.

The excess entropy gives information on the order of the mixed state in relation to the order of an ideal mixed state. A positive excess entropy value is an indication that the mixed state is more disordered than the ideal mixed state for which only the configurational disorder is computed. This is the general case for the mixed crystals. Nevertheless, the negative value of the excess entropy is an indication of ordering on mixing. The main question arises as to what kind of short-range order (conformational, orientational, etc.) will be superimposed on the inherent disorder of configuration in these binary mixtures. The subject matter may be examined in light of dielectric spectroscopy. According to the general statement, the static permittivity in a fully ordered phase is low, whereas in disordered phases, large values have to be expected. $\Delta\epsilon$ can provide information about the short-range correlation in a mixture at constant temperature with regard to the ideal mechanical mixture. As can be observed in Figure 8, the $\Delta\epsilon$ for the mixtures is always lower than the $\Delta\epsilon$ of the ideal mechanical mixture; that is to say that the excess dielectric strength ($\Delta\epsilon^{EX} = \Delta\epsilon_{mix} - \Delta\epsilon_{mecmix}$) is negative, clearly indicating the formation of multimer structures in the mixture.[32−33] Therefore, short-range correlations in reorientational disorder might be expected. All of the related features of the excess properties of the OD mixed state are indeed singular, thus making the two-component system a unique system.

A few years ago, some of the authors of this paper published a log−log plot[31] (Figure 11) in which the plane of the mixed states (molecular, metallic, ionic) could be divided into two regions. The empty circles in Figure 11 represent mixed crystals of isolated two-component systems, and the solid symbols represent families (or groups) of mixed crystals. The horizontal extension of each mark is proportional to the mean temperature range of the various systems forming the group. The diagonal solid line, named the zero-excess Gibbs energy line, where the compensation temperature is the same as the mean temperature, divides the plane into two regions. The region above the diagonal line was named "ordinary" because most of the mixed states are located there. In this region, the compensation temperature is above the mean temperature at which the mixed state melts, and if we speak of the excess Gibbs energy, then the excess enthalpy contribution is dominant with regard to the excess entropy contribution ($T_mS^{E}(X = 0.5)$). Furthermore, the excess Gibbs energy has the same sign as the excess enthalpy.

On the contrary, the region below the zero-excess Gibbs energy line was named "extraordinary" because of the lack of mixed states located there. In such a region, the excess Gibbs

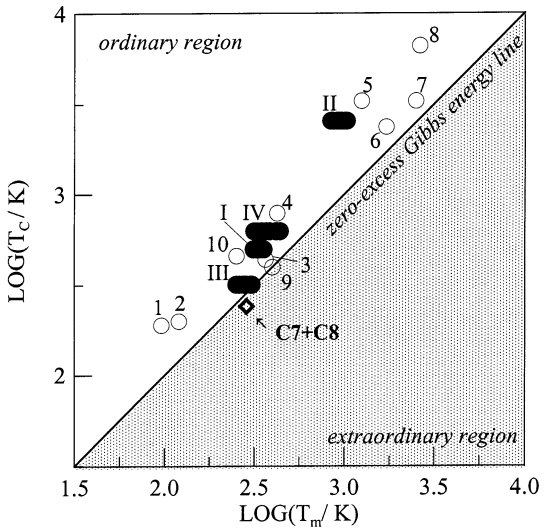


**Figure 11.** log−log representation of compensation temperature ($T_C$) versus equimolar EGC temperature or mean temperature ($T_m$) for given system or family. Empty circles are isolated systems: 1, Ar + Kr;[34] 2, Kr + Xe;[34] 3, D-carvoxime + L-carvoxime;[35] 4, 1,2,4,5-tetrachlorobenzene + 1,2,4,5-tetrabromobenzene;[36] 5, Ni + Au;[37] 6, Pd + Au;[38] 7, SrO + BaO;[39] 8, MgO + CaO;[39] 9, $CBr_4$ + $C_2Cl_6$;[40] 10, $CCl_4$ + $C(CH_3)_4$.[27] Solid symbols: I, *p*-dihalobenzene family;[41] II, common-ion alkali halide family;[42] III, *n*-alkane family;[43,44] IV, the class of neopentane derivatives.[31]

energy has the opposite sign to that of the excess enthalpy because the excess entropy contribution ($T_mS^E(X = 0.5)$) is dominant in relation to the excess enthalpy. This fact is not forbidden but occasionally occurs. The two-component system C7 + C8 is an extraordinary system because its OD mixed crystals are located in the extraordinary region in the log−log plot. In fact, it is the sole system as far as we know exhibiting extraordinary mixed crystals.

## 7. Concluding Remarks

The stable polymorphic behavior of both the C7 and C8 pure components has been analyzed in light of new thermal measurements as well as X-ray crystallographic measurements. From the latter, phase I of both pure components has been stated as simple cubic with similar lattice parameters. As for pure C8, only one other phase, phase II, has been observed above 170 K, and the lattice symmetry of that remains unknown. As for pure C7, in addition to phase I, two phases above 170 K have been observed to be stable: phase II, the lattice symmetry of which has been tentatively stated as tetragonal and phase III, the lattice symmetry of which remains unfortunately unknown because the X-ray patterns are not good enough.

However, the two-component system C7 + C8 has been stated. The binary mixtures are able to transform only into phase I, and they remain metastable at lower temperatures. From a crystallographic point of view, the SC states of C7 and C8 are related by an isomorphism relationship. From a thermodynamic point of view, the SC mixed state reveals a unique behavior (i.e., the excess enthalpy and excess entropy are negative whereas the excess Gibbs energy is positive). Likewise, they verify a compensation law with a compensation temperature ($T_c$) of about 242 K. In addition, the SC mixtures are classified as extraordinary in light of the log $T_c$−log $T_m$ plot.

**Acknowledgment.** This work was supported by the Spanish DGE under grant PB98-0923. We also acknowledge Professors M.A. Pérez-Jubindo and M.R. de la Fuente (Universidad del País Vasco) for providing access to the experimental facilities in which the dielectric measurements were performed.

## References and Notes

(1) Dworkin, A.; Fuchs, A. H.; Ghelfestein, M.; Szwarc, H. *J. Phys. Lett.* **1982**, *43*, L21.
(2) Edelman, R.; Würflinger, A. *Mol. Cryst. Liq. Cryst.* **1987**, *148*, 249.
(3) Shablakh, M.; Dissado, L. A.; Hill, R. M. *J. Chem. Soc., Faraday Trans.* **1983**, *79*, 383.
(4) Poser, U.; Würflinger, A. *Ber. Bunsen-Ges. Phys. Chem.* **1988**, *92*, 765.
(5) Würflinger, A. *Ber. Bunsen-Ges.Phys. Chem.* **1991**, *95*, 1040.
(6) Forsman, H.; Andersson, O. *J. Non-Cryst. Solids* **1990**, *131*−*133*, 1145.
(7) Leslie-Pelecky, D. L.; Birge, N. O. *Phys. Rev. Lett.* **1994**, *72*, 1232.
(8) Leslie-Pelecky, D. L.; Birge, N. O. *Phys. Rev. B* **1994**, *50*, 13250.
(9) Tyagi, M.; Murthy, S. S. N. *J. Chem. Phys*. **2001**, *114*, 3640.
(10) Sciescinsky, J.; Mayer, J.; Wasiutinsky, T.; Sciesinska, E.; Wojtowicz, J. *Phase Transitions* **1995**, *54*, 15.
(11) Andersson, O.; Ross, R. G. *Mol. Phys.* **1990**, *71*, 523.
(12) *CRC Handbook of Chemistry and Physics*, 54th ed.; CRC Press: Cleveland, OH, 1973−1974; p C-260.
(13) Fuchs, A. H.; Virlet, J.; André, D.; Szwarc, H. *J. Chim. Phys.* **1985**, *82*, 293.
(14) Sciesinska, E.; Sciescinsky, J. *Spectrosc. Lett.* **1990**, *23*, 293.
(15) Adachi, K.; Suga, H.; Seki, S. *Bull. Chem. Soc. Jpn.* **1972**, *45*, 1960.
(16) Poser, U.; Schulte, L.; Würflinger, A. *Ber. Bunsen-Ges. Phys. Chem.* **1985**, *89*, 1278.
(17) Pingel, N.; Poser, U.; Würflinger, A. *J. Chem. Soc., Faraday Trans.* **1984**, *80*, 3221.
(18) Courchinoux, R.; Chanh, N. B.; Haget, Y.; Calvet, T.; Estop, E.; Cuevas-Diarte, M. A. *J. Chim. Phys.* **1989**, *86*, 561.
(19) Barrio, M.; Font, J.; López, D. O.; Muntasell, J.; Tamarit, J. Ll; Chanh, N. B.; Haget, Y. *J. Chim. Phys.* **1990**, *87*, 2455.
(20) Ceballos, J. C.; Salud, J. Private communication.
(21) Louer, D.; Boultif, A. *DICVOL91*, Laboratoire de Cristallochemie: Université de Rennes I, France, 1992.
(22) Salud, J.; López, D. O.; Barrio, M.; Tamarit, J. Ll. *J. Mater. Chem.* **1999**, *9*, 909.
(23) Oonk, H. A. J. *Phase Theory: The Thermodynamics of Heterogeneous Equilibria*; Elsevier: Amsterdam, 1981.
(24) Daranas, D.; López, R.; López, D. O. *WINIFIT 2.0*; Polythecnical University of Catalonia: Barcelona, 2000.
(25) Jacobs, M. H. G.; Oonk, H. A. J. *LIQFIT: A Computer Program for the Thermodynamic Assessment of T*−*X Liquidus or Solidus Data*. Utrecht University: 1990,
(26) van Duijneveldt, J. S.; Baas, F. A. S.; Oonk, H. A. J. *PROPHASE: An MS-DOS Program for the Calculation of Binary T*−*X Phase Diagrams*; Utrecht University: Utrecht, The Netherlands, 1988.
(27) Salud, J.; López, D. O.; Tamarit, J. Ll.; Barrio, M.; Jacobs, M. H. G.; Oonk, H. A. J. *J. Solid State Chem.* **2000**, *154*, 390.
(28) Pardo, L. C.; Barrio, M.; Tamarit, J. Ll.; Negrier, P.; López, D. O.; Salud, J.; Mondieig, D. *J.Phys. Chem. B* **2001**, *105*, 10326.
(29) Sied, M. B.; López, D. O.; Tamarit, J. Ll.; Barrio, M. *Liq. Cryst.* **2002**, *29*, 57.
(30) Salud, J.; López, D. O.; Barrio, M.; Tamarit, J. Ll.; Oonk, H. A. J.; Negrier, P.; Haget, Y. *J. Solid State Chem.* **1997**, *133*, 536.
(31) López, D. O.; Salud, J.; Tamarit, J. Ll.; Barrio, M.; Oonk, H. A. J. *Chem. Mater.* **2000**, *12*, 1108.
(32) Shirke, R. M.; Chaudhari, A.; More, N. M.; Patil, P. B. *J. Mol. Liq.* **2001**, *94*, 27.
(33) Pawar, V. P.; Mehrotra, S. C. *J. Mol. Liq.* **2001**, *95*, 63.
(34) Walling, J. F.; Halsey, G. D. *J. Phys. Chem*. **1958**, *62*, 756.
(35) Calvet, M. T.; Oonk, H. A. J. *CALPHAD* **1995**, *19*, 49.
(36) Van Genderen, M. J.; Mondieig, D.; Haget, Y.; Cuevas-Diarte, M. A.; Oonk, H. A. J. *CALPHAD* **1992**, *16*, 301.
(37) Sellers, C. M.; Maak, F. *Trans. Metall. Soc. AIME* **1966**, *236*, 457.
(38) Okamoto, H.; Massalsky, T. B. *Bull. Alloy Phase Diagrams* **1985**, *6*, 229.
(39) Van der Kemp, W. J. M.; Blok, J. G.; Van der Linde, P. R.; Oonk, H. A. J.; Schuijff, A.; Verdonk, M. L. *CALPHAD* **1994**, *18*, 225.
(40) Van Braak, J.; López, D. O.; Salud, J.; Tamarit, J. Ll.; Jacobs, M. H. G.; Oonk, H. A. J. *J. Cryst. Growth* **1997**, *180*, 315.
(41) Calvet, M. T.; Cuevas-Diarte, M. A.; Haget, Y.; Van der Linde, P. R.; Oonk, H. A. J. *CALPHAD* **1991**, *15*, 225.
(42) Van der Kemp, W. J. M.; Blok, J. G.; Van Genderen, A. C. G.; Van Ekeren, P. J.; Oonk, H. A. J. *Thermochim. Acta* **1992**, *196*, 301.
(43) Oonk, H. A. J.; Mondieig, D.; Haget, Y.; Cuevas-Diarte, M. A. *J. Chem. Phys.* **1998**, *108*, 715.
(44) Mondieig, D.; Espeau, P.; Robles, L.; Haget, Y.; Oonk, H. A. J.; Cuevas-Diarte, M. A. *J. Chem. Soc., Faraday Trans.* **1997**, *93*, 3343.